Inorganic Chemistry
Article

Inorg. Chem. **2011**, *50*, 1339–1350 **1339**
DOI: 10.1021/ic1018423

Diorganotin-Based Coordination Polymers Derived from Sulfonate/Phosphonate/Phosphonocarboxylate Ligands

Ravi Shankar,*,† Archana Jain,† Gabriele Kociok-Köhn,‡ and Kieran C. Molloy‡

†*Department of Chemistry, Indian Institute of Technology, Hauz Khas, New Delhi 110016, India, and*
‡*Department of Chemistry, University of Bath, Bath BA2 7AY, U.K.*

Received September 8, 2010

The reactions of diorganotin precursors $[R_2Sn(OR^1)(OSO_2R^1)]_n$ [R = R^1 = Me (**1**); R = Me, R^1 = Et (**2**)] with an equimolar amount of *t*-butylphosphonic acid (RT, 8−10 h) in methanol result in the formation of identical products, of composition $[(Me_2Sn)_3(O_3PBu^t)_2(O_2P(OH)Bu^t)_2]_n$ (**3**). On the other hand, a similar reaction of **2**, when carried out in dichloromethane, affords $[(Me_2Sn)_3(O_3PBu^t)_2(OSO_2Et)_2 \cdot MeOH]_n$ (**4**). A plausible mechanism implicating the role of solvent in the formation of these compounds has been put forward. In addition, the synthesis of $[(Me_2Sn)_3(O_3PCH_2CH_2COOMe)_2(OSO_2Me)_2]_n$ (**5**) and $[R_2Sn(O_2P(OH)CH_2CH_2COOMe)(OSO_2R^1)]_n$ [R = Et, R^1 = Me (**6**); R = ^{n}Bu, R^1 = Et (**7**)] has been achieved by reacting **1** and related diorganotin(alkoxy)alkanesulfonates with 3-phosphonopropionic acid in methanol. The formation of a methylpropionate functionality on the phosphorus center in these structural frameworks results from in situ esterification of the carboxylic group. X-ray crystallographic studies of **1**−**7** are presented. The structures of **1** and **2** represent one-dimensional (1D) coordination polymers composed of alternate $[Sn-O]_2$ and $[Sn-O-S-O]_2$ cyclic rings formed by μ_2-alkoxo and sulfonate ligands, respectively. For **3**−**5** and **7**, variable bonding modes of phosphonate and/or sulfonate ligands afford the construction of two- and three-dimensional self-assemblies that are comprised of trinuclear tin entities with an $Sn_3P_2O_6$ core as well as $[Sn-O-P-O]_2$ and/or $[Sn-O-S-O]_2$ rings. The formation of a 1D coordination polymer in **6** is unique in terms of repeating eight-membered cyclic rings containing Sn, O, P, and S heteroatoms. The contribution from hydrogen-bonding interactions is also found to be significant in these structures.

Introduction

The coordination chemistry of phosphonate RPO_3^{2-}/$RP(OH)O_2^-$ and related bifunctional anionic ligands such as carboxyphosphonates, $X(CH_2)_nPO_3^{2-}$ (X = CO_2^- or COOH; n = 2 or 3) with transition-metal elements has witnessed an exponential growth due to potential applications of these compounds in catalysis, ion-exchange, sorption, sensors, intercalation, and materials research.[1−3] These studies have provided fundamental insights into the ubiquitous bonding behavior of these ligands toward different metal ions and their role in the construction of porous metal−organic frameworks. On the other hand, analogous studies in main-group chemistry are scarce.[4] In this latter area, much of the current efforts have been devoted to the development of synthetic methods for group 13-based (B, Al, Ga, and In) metal phosphonates and their structural elucidation by X-ray crystallography.[1c] A general synthetic approach for these compounds involves the reaction of trialkylmetal precursors with an appropriate phosphonic acid. The facile cleavage of an M−C bond and elimination

*To whom correspondence should be addressed. E-mail: shankar@chemistry.iitd.ac.in.

(1) (a) Simizu, G. K. H.; Ramanathan, V.; Taylor, J. M. *Chem. Soc. Rev.* **2009**, *38*, 1430. (b) Clearfield, A. *Progress in Inorganic Chemistry: Metal Phosphonate Chemistry*; Karlin, K. D., Ed.; John Wiley & Sons: New York, 1998; Vol. *47*, p 371. (c) Walawalker, M. G.; Roesky, H. W.; Murugaval, R. *Acc. Chem. Res.* **1999**, *32*, 117. (d) Mallouk, T. E.; Kim, H. N.; Olliver, P. J.; Keller, S. W. In *Comprehensive Supramolecular Chemistry*; Alberti, G., Bein, T., Eds.; Pergamon: New York, 1996; Vol. *7*, p 189. (e) Cao, G.; Hong, H.-G.; Mallouk, T. E. *Acc. Chem. Res.* **1992**, *25*, 420. (f) Singleton, R.; Bye, J.; Dyson, J.; Baker, G.; Ranson, R. M.; Hix, G. B. *Dalton Trans.* **2010**, *39*, 6024. (g) Thompson, M. E. *Chem. Mater.* **1994**, *6*, 1168.

(2) (a) Nonglaton, G.; Benitez, I. O.; Guisle, I.; Pipeler, M.; Leger, J.; Dubreuil, D.; Tellier, C.; Talham, D. R.; Bujoli, B. *J. Am. Chem. Soc.* **2004**, *126*, 1497. (b) Deniaud, D.; Schollorn, B.; Mansury, J.; Rouxel, J.; Battion, P.; Bujoli, B. *Chem. Mater.* **1995**, *7*, 995. (c) Hu, A.; Ngo, H.; Lin, W. *J. Am. Chem. Soc.* **2003**, *125*, 11490. (d) Hu, A.; Yee, G. T.; Lin, W. *J. Am. Chem. Soc.* **2005**, *127*, 12486. (e) Zhu, J.; Bu, X.; Feng, P.; Stucky, G. D. *J. Am. Chem. Soc.* **2000**, *122*, 11563. (f) Wang, J. D.; Clearfield, A.; Peng, G.-Z. *Mater. Chem. Phys.* **1993**, *35*, 208. (g) Alberti, G. In *Comprehensive Supramolecular Chemistry*; Alberti, G., Bein, T., Eds.; Pergamon: New York, 1996; Vol. *7*, p 151. (h) Maeda, K.; Kiyozumi, Y.; Mizukami, F. *J. Phys. Chem. B* **1997**, *101*, 4402. (i) Fredoueil, F.; Massiot, D.; Janvier, P.; Gingl, F.; Bujoli-Doeuff, M.; Evian, M.; Clearfield, A.; Bujoli, B. *Inorg. Chem.* **1999**, *8*, 1831. (j) Maeda, K. *Microporous Mesoporous Mater.* **2004**, *73*, 47. (k) Miller, S. R.; Pearce, G. M.; Wright, P. A.; Bonino, F.; Chavan, S.; Bordiga, S.; Margiolaki, I.; Guillou, N.; Férey, G.; Bourrelly, S.; Llewellyn, P. L. *J. Am. Chem. Soc.* **2008**, *130*, 15967. (l) Sanchez-Moreno, M. J.; Fernandez-Botello, A.; Gomez-Coca, R. B.; Griesser, R.; Ochocki, J.; Kotynski, A.; Niclos-Gutierrez, J.; Moreno, V.; Sigel, H. *Inorg. Chem.* **2004**, *43*, 1311. (m) Du, Z.-Y.; Xu, H.-B.; Mao, J.-G. *Inorg. Chem.* **2006**, *45*, 6424. (n) Poojary, D. M.; Clearfield, A. *J. Am. Chem. Soc.* **1995**, *117*, 11278. (o) Zhang, Y.; Clearfield, A. *Inorg. Chem.* **1992**, *31*, 2821. (p) Cao, G.; Lynch, V. M.; Yacullo, L. N. *Chem. Mater.* **1993**, *5*, 1000.

Published on Web 01/20/2011

Scheme 1

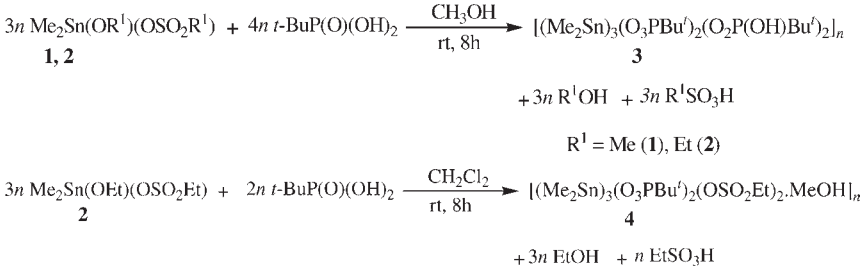

of alkane as a byproduct make this procedure quite attractive. Richards et al.[5] have recently reported that the reaction of trivalent metal chlorides with a phosphonic acid also provides access to analogous metal phosphonates. Nevertheless, organotin phosphonates are generally known to be associated with an insoluble nature, often precipitating as less ordered solid phases. There are only a few structurally known examples among this family and include homoleptic $[^{n}Bu_2Sn(OP(O)(OH)Me)_2]_2$[6a] (dimer), $[Me_3Sn(OP(O)(OH)Ph)]_n$[6b] (helical polymer), $[(^{n}BuSn)_2O(OP(O)(OH)^{t}Bu)_4]_2$[6c] (cluster), and $[Na_6(CH_3OH)_2(H_2O)][\{(BzSn)_3(PhPO_3)_5(\mu_3\text{-}O)(CH_3O)\}_2\text{-}Bz_2Sn]CH_3OH$[6d] (oligomer).

Studies on the coordination aspects of phosphonoacetic/propionic acid, $HO_3P(CH_2)_nCO_2H$ (n = 2, 3), toward main-group metal ions such as Al^{III}, Ga^{III}, and Pb^{II} are emerging.[7] The synthesis of these metal phosphonocarboxylates has been achieved by a hydrothermal method. Following this approach, Cheetham et al.[8] have recently reported a hybrid open framework of tin(II) phosphonopropionateoxalate, $Sn_4(O_3PCH_2CH_2CO_2)_2(C_2O_4)$. These studies have revealed that the final stoichiometry of the resulting products is strongly governed by the degree of deprotonation of the phosphonic and carboxylic groups, which exhibit individual acid dissociation constants (pK_1 = ~2.0; pK_2 = 8.69; pK = 5.11)[9] that are separated from each other by several pH units, thus making it possible to tune their coordination behavior with metal ions.

We have recently reported synthetic and structural features of several diorganotin-based two- (2D) and three-dimensional (3D) coordination assemblies by incorporating both sulfonate and phosphonate ligands in the secondary building units (SBUs).[10] A salient feature of these self-assemblies is that they are composed of $[Sn-O-S-O]_2$ and $[Sn-O-P-O]_2$ rings as well as trinuclear tin entities such as $[(R_2Sn)_3(O_3PR^1)_2]$ (R = Me, Et; R^1 = Me, ^{t}Bu). The synthetic protocol involves the reaction of a mixed-ligand diorganotin(alkoxy)alkanesulfonate precursor, $[R_2Sn(OR^1)(OSO_2R^1)]_n$ (R = ^{n}Bu, R^1 = Me, Et, ^{n}Pr; R = R^1 = Me, Et) with an appropriate phosphonic acid (RT, CH_2Cl_2, 8−10 h). The modular nature of a weakly coordinating sulfonate ligand via μ_1, μ_2, and μ_3 modes and its role in the execution of CH−O-type hydrogen bonding are particularly noticeable during the self-assembly process. As a part of our continued interest in this area, we sought to explore synthetic possibilities to alter the functionalities on the SBUs, with emphasis on utilizing their coordination abilities in the construction of higher-dimensional organotin-based coordination polymers. Herein, we describe the synthesis of a few SBUs, $[(R_2Sn)_3(O_3PR^1)_2L_2]$ [L = $O_2P(OH)Bu^{t}$, OSO_2Et] featuring appended hydrogenphosphonate or sulfonate groups on the trinuclear tin phosphonate core and formation of new 3D structural motifs derived therefrom (**3** and **4**). In addition, the use of 3-phosphonopropionic acid as the directing ligand allows the isolation of functional coordination polymers, $[(Me_2Sn)_3(O_3PCH_2CH_2COOMe)_2(OSO_2\text{-}Me)_2]_n$ (**5**) and $[R_2Sn(O_2P(OH)CH_2CH_2COOMe)(OSO_2R^1)]_n$ [R = Et, R^1 = Me (**6**); R = ^{n}Bu, R^1 = Et (**7**)] bearing an appended ester functionality on the phosphonate ligand.

Results and Discussion

Synthetic Aspects. The synthesis of diorganotin(alkoxy)-alkanesulfonates being used herein was reported earlier.[10] The reactions between equimolar quantities of the precursor tin complexes, $[Me_2Sn(OR^1)(OSO_2R^1)]_n$ [R^1 = Me (**1**), Et (**2**)], and *tert*-butylphosphonic acid in methanol afford products of identical composition, $[(Me_2Sn)_3\text{-}(O_3PBu^{t})_2(O_2P(OH)Bu^{t})_2]_n$ (**3**). On the other hand, a similar reaction of **2** with phosphonic acid, when performed

(3) (a) Bhardwaj, C.; Hu, H.; Clearfield, A. *Inorg. Chem.* **1993**, *32*, 4294. (b) Chandrasekhar, V.; Senapati, T.; Sanudo, E. C. *Inorg. Chem.* **2008**, *47*, 9553. (c) Gómez-Alcantara, M. M.; Aranda, M. A. G.; Olivera-Pastor, P.; Beran, P.; García-Muñoz, J. L.; Cabeza, A. *Dalton Trans.* **2006**, 577. (d) Drumel, S.; Janvier, P.; Barboux, P.; Bujoli-Doeuff, M.; Bujol, B. *Inorg. Chem.* **1995**, *34*, 148. (e) Distler, A.; Sevov, S. C. *Chem. Commun.* **1998**, 959. (f) Sabbar, E. M.; de Roy, M. E.; Ennaqadi, A.; Gueho, C.; Besse, J. P. *Chem. Mater.* **1998**, *10*, 3856. (g) Stock, N.; Frey, S. A.; Stucky, G. D.; Cheetham, A. K. *J. Chem. Soc., Dalton Trans.* **2000**, 4292. (h) Riou-Cavellec, M.; Sanselme, M.; Grenèche, J.-M.; Férey, G. *Solid State Sci.* **2000**, *2*, 717. (i) Fredoueil, F.; Evain, M.; Massiot, D.; Bujoli-Doeuff, M.; Janvier, P.; Clearfield, A.; Bujoli, B. *J. Chem. Soc., Dalton Trans.* **2002**, 1508.

(4) (a) Mason, M. R. *J. Cluster Sci.* **1998**, *9*, 1. (b) Maeda, K.; Akimoto, J.; Kiyozumi, Y.; Mizukami, F. *Chem. Commun.* **1995**, 1033. (c) Maeda, K.; Akimoto, J.; Kiyozumi, Y.; Mizukami, F. *Angew. Chem., Int. Ed.* **1995**, *34*, 1199. (d) Bujoli-Doeuff, M.; Evain, M.; Fayon, F.; Alonso, B.; Massiot, D.; Bujoli, B. *Eur. J. Inorg. Chem.* **2000**, 2497. (e) Mason, M. R.; Mashuta, M. S.; Richardson, J. F. *Angew. Chem., Int. Ed. Engl.* **1997**, *36*, 239. (f) Keys, A.; Bott, S.; Barron, A. R. *Chem. Commun.* **1996**, 2339. (g) Walawalker, M. G.; Murugaval, R.; Roesky, H. W.; Scmidt, H.-G. *Inorg. Chem.* **1997**, *36*, 4202.

(5) Samanamu, C. R.; Olmstead, M. M.; Montchamp, J.-L.; Richards, A. F. *Inorg. Chem.* **2008**, *47*, 3879.

(6) (a) Ribot, F.; Sanchez, C.; Biesemans, M.; Mercier, F. A. G.; Martins, J. C.; Gielen, M.; Willem, R. *Organometallics* **2001**, *20*, 2593. (b) Molloy, K. C.; Hossain, M. B.; van der Helm, D.; Cunningham, D.; Zuckerman, J. J. *Inorg. Chem.* **1981**, *20*, 2402. (c) Kumara Swamy, K. C.; Schmid, C. G.; Day, R. O.; Holmes, R. R. *J. Am. Chem. Soc.* **1990**, *112*, 223. (d) Song, S.-Y.; Ma, J.-F.; Yang, J.; Gao, L.-L.; Su, Z.-M. *Organometallics* **2007**, *26*, 2125.

(7) (a) Hix, G. B.; Wragg, D. S.; Wright, P. A.; Morris, R. E. *J. Chem. Soc., Dalton Trans.* **1998**, 3359. (b) Fredoueil, F.; Massiot, D.; Poojary, D.; Bujoli-Doeuff, M.; Clearfield, A.; Bujoli, B. *Chem. Commun.* **1998**, 175. (c) Ayyappan, S.; de Delgado, G. D.; Cheetham, A. K.; Férey, G.; Rao, C. N. R. *J. Chem. Soc., Dalton Trans.* **1999**, 2905.

(8) Stock, N.; Stucky, G. D.; Cheetham, A. K. *Chem. Commun.* **2000**, 2277.

(9) Heubel, P.-H. C.; Popov, A. I. *J. Solution Chem.* **1979**, *8*, 615.

(10) (a) Shankar, R.; Singh, A. P.; Upreti, S. *Inorg. Chem.* **2006**, *45*, 9166. (b) Shankar, R.; Singh, A. P.; Jain, A.; Mahon, M. F.; Molloy, K. C. *Inorg. Chem.* **2008**, *47*, 5930. (c) Shankar, R.; Jain, A.; Singh, A. P.; Kociok-Köhn, G.; Molloy, K. C. *Inorg. Chem.* **2009**, *48*, 3608. (d) Shankar, R.; Jain, A.; Kociok-Köhn, G.; Mahon, M. F.; Molloy, K. C. *Inorg. Chem.* **2010**, *49*, 4708.

Table 1. Summary of the Crystallographic Data for **1**−**7**

crystal data	**1**	**2**	**3**	**4**	**5**	**6**	**7**
empirical formula	$C_8H_{24}O_8S_2Sn_2$	$C_6H_{16}O_4SSn$	$C_{22}H_{56}O_{12}P_4Sn_3$	$C_{19}H_{50}O_{13}P_2S_2Sn_3$	$C_{16}H_{32}O_{16}P_2S_2Sn_3$	$C_9H_{21}O_8PSSn$	$C_{14}H_{31}O_8PSSn$
fw	549.77	302.94	992.62	968.72	962.55	438.98	509.11
λ, Å	0.710 73	0.710 73	0.710 73	0.710 73	0.710 73	0.710 73	0.710 73
cryst syst	monoclinic	triclinic	monoclinic	monoclinic	tetragonal	monoclinic	monoclinic
space group	$P2_1/n$	$P\bar{1}$	$P2_1/c$	$P2_1/c$	$P4_122$	$P2_1$	$C2/c$
a, Å	8.1679(2)	7.5018(3)	14.4812(2)	13.35850(10)	10.61360(10)	5.3471(3)	31.4648(6)
b, Å	7.4189(2)	8.3606(3)	14.9061(2)	15.4326(2)	10.61360(10)	35.9423(11)	9.9269(2)
c, Å	14.3586(5)	8.9734(3)	18.8064(2)	17.3314(2)	28.72110(10)	8.7245(4)	16.5748(4)
α, deg		76.613(2)					
β, deg	92.5920(10)	88.689(2)	104.5790(10)	96.4740(10)		106.483(2)	120.4520(10)
γ, deg		86.0330(10)					
V, Å^3	869.20(4)	546.19(3)	3928.80(9)	3550.19(7)	3235.39(4)	1607.83(13)	4462.94(16)
Z	2	2	4	4	4	4	8
ρ_{calcd}, Mg m^{-3}	2.101	1.842	1.678	1.812	1.976	1.813	1.515
μ, mm^{-1}	3.141	2.509	2.102	2.353	2.589	1.848	1.343
F(000)	536	300	1976	1920	1872	880	2080
cryst size, mm	0.15 × 0.15 × 0.10	0.25 × 0.10 × 0.08	0.25 × 0.15 × 0.10	0.20 × 0.20 × 0.20	0.25 × 0.20 × 0.20	0.25 × 0.25 × 0.03	0.30 × 0.20 × 0.05
θ, deg	2.93−27.45	3.01−30.09	3.10−27.52	2.96−30.05	3.84−30.06	3.97−27.48	3.28−27.51
limiting indices	$-10 \le h \le 10$; $-9 \le k \le 9$; $-18 \le l \le 18$	$-10 \le h \le 10$; $-11 \le k \le 11$; $-12 \le l \le 12$	$-18 \le h \le 18$; $-19 \le k \le 19$; $-23 \le l \le 24$	$-18 \le h \le 18$; $-21 \le k \le 21$; $-24 \le l \le 24$	$-14 \le h \le 14$; $-14 \le k \le 14$; $-40 \le l \le 40$	$-6 \le h \le 6$; $-35 \le k \le 46$; $-10 \le l \le 11$	$-40 \le h \le 39$; $-12 \le k \le 12$; $-21 \le l \le 21$
reflns colld	10 299	11 099	56 456	66 075	46 641	6656	29 771
indep reflns	1984	3209	8988	10 383	4736	3668	5111
data completeness	0.997	0.994	0.995	0.997	0.995	0.681	0.994
max and min transmn	0.7292 and 0.6371	0.8245 and 0.5728	0.8173 and 0.6215	0.6244 and 0.6244	0.9359 and 0.6888	0.9359 and 0.6888	0.9359 and 0.6888
R(int)	0.0374	0.0616	0.0574	0.0572	0.1679	0.0609	0.0462
GOF on F^2	1.077	1.068	1.089	1.108	1.070	1.042	1.088
data/restraints/param	1984/0/95	3209/0/113	8988/0/390	10383/1/371	4736/0/181	3668/1/372	5111/0/230
final R indices [$I > 2\sigma(I)$]	R1 = 0.0298, wR2 = 0.0653	R1 = 0.0340, wR2 = 0.0690	R1 = 0.0292 wR2 = 0.0611	R1 = 0.0383, wR2 = 0.0853	R1 = 0.0428, wR2 = 0.0942	R1 = 0.0453, wR2 = 0.1009	R1 = 0.0300, wR2 = 0.0694
R indices (all data)	R1 = 0.0399, wR2 = 0.0700	R1 = 0.0482, wR2 = 0.0738	R1 = 0.0422 wR2 = 0.0660	R1 = 0.0568, wR2 = 0.0923	R1 = 0.0556, wR2 = 0.0994	R1 = 0.0572, wR2 = 0.1070	R1 = 0.0374, wR2 = 0.0740
largest diff peak and hole, e Å^{-3}	1.119 and −0.954	1.134 and −2.225	0.748 and −1.058	1.586 and −1.317	1.254 and −1.790	0.836 and −1.023	1.119 and −1.005

Table 2. Selected Bond Lengths (Å) and Bond Angles (deg) for **1**[a]

Sn−C3	2.097(4)	Sn−C2	2.110(4)
Sn−O1	2.116(3)	Sn−O1^{i}	2.153(2)
Sn−O3^{ii}	2.350(3)	Sn−O2	2.419(3)
C3−Sn−C2	160.04(17)	O1−Sn−O1^{i}	73.62(11)
O1−Sn−O3^{ii}	84.66(10)	O1^{i}−Sn−O2	89.75(9)
O3^{ii}−Sn−O2	111.87(10)		

[a] Symmetry transformations used to generate equivalent atoms: i, $-x$, $2-y$, $-z$; ii, $1-x$, $2-y$, $-z$.

Table 3. Selected Bond Lengths (Å) and Bond Angles (deg) for **2**[a]

Sn−C6	2.093(3)	Sn−C5	2.100(3)
Sn−O4	2.121(2)	Sn−O4^{i}	2.1418(19)
Sn−O1	2.324(2)	Sn−O2^{ii}	2.415(2)
C6−Sn−C5	161.27(13)	O4−Sn−O4^{i}	72.69(9)
O4−Sn−O1	85.89(7)	O4^{i}−Sn−O2^{ii}	91.25(7)
O1−Sn−O2^{ii}	110.16(7)		

[a] Symmetry transformations used to generate equivalent atoms: i, $-x+1$, $-y+1$, $-z$; ii, $-x+1$, $-y$, $-z$.

Table 4. Selected Bond Lengths (Å) and Bond Angles (deg) for **3**[a]

Sn1−O1	2.0121(19)	Sn1−O7	2.151(2)
Sn1−O4	2.215(2)	Sn1−C1	2.109(3)
Sn1−C2	2.110(3)	Sn2−O5	2.023(2)
Sn2−O12^{i}	2.127(2)	Sn2−O2	2.150(2)
Sn2−C4	2.109(3)	Sn2−C3	2.115(3)
Sn3−O6	2.0284(19)	Sn3−O3	2.162(2)
Sn3−O10	2.176(2)	Sn3−C5	2.103(3)
Sn3−C6	2.107(3)		
O7−Sn1−O4	166.72(8)	O1−Sn1−C1	100.30(10)
O1−Sn1−C2	125.38(11)	C1−Sn1−C2	134.26(13)
O12^{i}−Sn2−O2	173.52(9)	O5−Sn2−C4	106.25(11)
O5−Sn2−C3	115.47(12)	C4−Sn2−C3	138.20(15)
O3−Sn3−O10	174.54(8)	O6−Sn3−C5	105.80(11)
O6−Sn3−C6	110.96(10)	C5−Sn3−C6	142.92(13)

[a] Symmetry transformations used to generate equivalent atoms: i, $-x+1$, $y+{}^{1}/_{2}$, $-z+{}^{1}/_{2}$.

in dichloromethane, affords precipitation of a white solid, which upon crystallization from a chloroform−methanol mixture yields $[(Me_2Sn)_3(O_3PBu^t)_2(OSO_2Et)_2\cdot MeOH]_n$ (**4**) bearing both sulfonate and phosphonate ligand sets in the framework structure (Scheme 1).

It is significant to note that solvent effects play a pivotal role for different reactivity behaviors of the tin precursors **1** and **2** toward phosphonic acid. The formation of **4** in a dichloromethane medium is viewed as resulting from the slow precipitation of the compound during the course of the reaction. An analogous result from the reaction of **1** with *tert*-butylphosphonic acid was recently reported by us, and a plausible pathway involving mixed-ligand diorganotin species, $[Me_2Sn(O_2P(OH)Bu^t)(OSO_2Me)]_n$ (n = 1, 2), has been invoked to rationalize the formation of the trinuclear tin phosphonate assembly, with two of its Sn atoms bearing an appended sulfonate group.[10c] On the other hand, the formation of **3** in a methanolic medium involves **4** as the intermediate, and preferential solubility of the latter in methanol allows its subsequent transformation by ligand exchange between the peripheral sulfonate ligands and phosphonic acid. Further validation of this intermediate has been sought by the direct reaction of **4** with *tert*-butylphosphonic acid in methanol, which has resulted in the isolation of **3** in moderate yields.

The mixed-ligand tin complex **1** reacts readily with an equimolar quantity of 3-phosphonopropionic acid in methanol (RT, 8−10 h) to afford a white solid, which upon slow crystallization from an acetonitrile−methanol−diethyl ether mixture yields a crop of crystals of composition $[(Me_2Sn)_3(O_3PCH_2CH_2COOMe)_2(OSO_2Me)_2]_n$ (**5**).

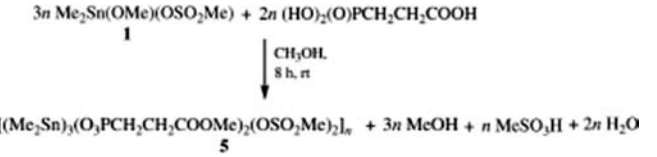

Analogous reactions with other tin precursors $[R_2Sn(OR^1)(OSO_2R^1)]_n$ proceed via selective substitution of the alkoxy group, resulting in the isolation of $[R_2Sn(O_2P(OH)CH_2CH_2COOMe)(OSO_2R^1)]_n$ [R = Et, R^1 = Me (**6**); R = ^{n}Bu, R^1 = Et (**7**)].

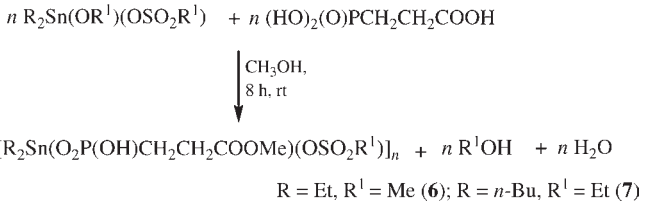

It is significant to note the in situ transformation of the free carboxylic group into an ester moiety, which remains an integral part of the structural frameworks of **5**−**7**. From a mechanistic viewpoint, it is believed that the formation of a methyl ester moiety proceeds under acid-catalyzed conditions, which are provided by the dissociation of phosphonic acid (pK_1 = ∼2.0).[9] An alternate pathway involving an organotin-mediated esterification reaction has not been considered in view of a recent report[11] that provides evidence in favor of the in situ generation of an acid that functions as a catalyst in these reactions.

Crystallographic Studies. Single crystals suitable for X-ray crystallography were grown from a solution in methanol (for **3**), diethyl ether−chloroform−methanol (for **4**), and diethyl ether−acetonitrile−methanol (for **5**−**7**). The crystal data of **1**−**7** are summarized in Table 1, while selected bond lengths and angles are given in Tables 2−8, respectively.

The structural motifs of dimethyltin(alkoxy)alkanesulfonates **1** and **2** have been unequivocally established for the first time by X-ray crystallography. The asymmetric units are isostructural and are comprised of a dimer formed by μ_2 coordination of the alkoxide group (Figures 1a and 2a). The appended sulfonate group on each Sn atom also acts in a μ_2 fashion [O3(S) (for **1**) and O2(S) (for **2**)] and results in the formation of one-dimensional (1D) polymeric chains (Figures 1b and 2a). The extended coordination assembly thus formed reveals a unique disposition of alternate four-membered $[Sn-O]_2$ and eight-membered $-[Sn-O-S-O-]_2$ cyclic rings. The geometry around each Sn atom is a distorted octahedron with a planar SnO_4 core occupying the equatorial position [$\Sigma 360 \pm 0.10°$ (for **1**)/$360 \pm 0.01°$ (for **2**)]. The methyl groups on

(11) Crawford, E.; Lohr, T.; Leitao, E. M.; Kwok, S.; McIndoe, J. S. *Dalton Trans.* **2009**, 9110.

Table 5. Selected Bond Lengths (Å) and Bond Angles (deg) for **4**[a]

Sn1−O5	2.075(3)	Sn1−C1	2.085(4)
Sn1−O3	2.086(3)	Sn1−C2	2.094(4)
Sn1−O13	2.504(3)	Sn1−O12^{iii}	2.578(3)
Sn2−O1	2.060(2)	Sn2−C3	2.088(4)
Sn2−O4	2.091(2)	Sn2−C4	2.095(4)
Sn2−O7	2.439(3)	Sn2−O9^{iv}	2.777(3)
Sn3−O6	2.077(3)	Sn3−O2	2.081(2)
Sn3−C6	2.088(4)	Sn3−C5	2.099(4)
Sn3−O10	2.542(3)	Sn3−O8^{i}	2.559(3)
C1−Sn1−C2	152.00(17)	O5−Sn1−O3	92.06(10)
O3−Sn1−O13	78.27(11)	O12^{iii}−Sn1−O13	108.01(11)
O12^{iii}−Sn1−O5	81.91(10)	O1−Sn2−O4	90.77(10)
C3−Sn2−C4	149.35(16)	O1−Sn2−O7	80.76(10)
O4−Sn2−O9^{iv}	83.99(9)	O9^{iv}−Sn2−O7	105.36(9)
C6−Sn3−C5	156.35(16)	O6−Sn3−O2	90.50(10)
O6−Sn3−O10	91.14(12)	O2−Sn3−O8^{i}	82.35(10)
O10−Sn3−O8^{i}	96.07(12)		

[a] Symmetry transformations used to generate equivalent atoms: i, $-x$, $y + {}^1/_2$, $-z + {}^1/_2$; iii, $-x + 1$, $y - {}^1/_2$, $-z + {}^1/_2$; iv, $-x$, $-y$, $-z$.

Table 6. Selected Bond Lengths (Å) and Bond Angles (deg) for **5**[a]

Sn1−O1	2.097(3)	Sn1−O2^{i}	2.058(3)
O2−Sn1^{i}	2.058(3)	Sn2−O3	2.081(3)
Sn2−O3^{i}	2.081(3)	Sn1−O7^{ii}	2.362(4)
O7−Sn1^{iii}	2.362(4)	Sn2−O6^{i}	2.556(4)
Sn2−O6	2.556(4)	Sn1−C1	2.079(5)
Sn1−C2	2.087(5)	Sn2−C7	2.084(5)
Sn2−C7^{i}	2.084(5)	O5−C6	1.457(8)
C1−Sn1−C2	150.2(2)	O2^{i}−Sn1−C1	99.12(19)
O2^{i}−Sn1−C2	107.63(18)	O1−Sn1−O7^{ii}	168.42(15)
C7−Sn2−C7^{i}	149.1(3)	O3−Sn2−O3^{i}	91.21(19)
O3−Sn2−O6^{i}	79.54(13)	O3^{i}−Sn2−O6	79.54(13)
O6^{i}−Sn2−O6	110.61(17)		

[a] Symmetry transformations used to generate equivalent atoms: i, $-x + 1$, $-y + 1$, $-z + {}^1/_4$; ii, $-y$, $-x + 1$, $-z + {}^1/_4$.

the Sn atoms adopt a trans disposition with average C−Sn−C angles of 160.04(17)° (for **1**) and 161.27(13)° (for **2**). The Sn−O bond lengths derived from alkoxy and alkanesulfonate groups lie in the ranges of 2.11−2.16/2.35−2.41 Å (**1**) and 2.12−2.15/2.33−2.42 Å (**2**) and correlate well with those observed previously for related homoleptic diorganotin derivatives.[12] Despite the structural similarities, a marked variation between **1** and **2** is discernible with respect to the hydrogen-bonding interactions. For **1**, the polymeric chains are associated with one another by strong CH---O hydrogen bonds involving H4A and O4 atoms of methanesulfonate groups [C4−H4A = 0.980 Å, H4A---O4 = 2.528(3) Å, and C4---O4 = 3.493(5) Å; C4−H4A---O4 = 168.1(2)°; symmetry code, $-x + {}^1/_2$, $y - {}^1/_2$, $-z - {}^1/_2$] and direct the 1D coordination polymer into a 3D self-assembly (Figure 1c). On the other hand, hydrogen bonding between H1A and O3 atoms of ethanesulfonate groups provides a layered connectivity in **2** (Figure 2b). The metrical parameters [C1−H1A = 0.990 Å, H1A---O3 = 2.560(3) Å, and C1---O3 = 3.456(5) Å; C1−H1A---O3 = 150.4(1)°; symmetry code, $-x + 1$, $-y$, $-z + 1$] are consistent with those reported in the literature.[13]

The asymmetric unit of **3** (Figure 3a) represents a trinuclear tin moiety with a $Sn_3P_2O_6$ core, which is formed as a result of a μ_3-bonding mode of two dianionic phosphonate groups (P1 and P2). The structure is comprised of two fused eight-membered $-[Sn-O-P-O-]_2$ rings, with the Sn1 and Sn3 atoms being associated with covalently bonded hydrogenphosphonate groups (P3 and P4), respectively. Peripheral functionalization of the otherwise rigid tin phosphonate core framework with a $-O_2P(OH)Bu^t$ ligand allows coordinative association as well as hydrogen-bonding interactions between the SBUs and facilitates the formation of a 3D supramolecular assembly. Interestingly, the hydrogenphosphonate (P4) group is exclusive in its role to act as a μ_2-coordinating ligand, and its association with the Sn2 atom of an adjacent trinuclear tin phosphonate unit (via O12) extends the primary structure into a 1D coordination polymer along the *b* axis. Each Sn atom in this structural motif features a distorted trigonal-bipyramidal geometry with a planar SnC_2O core ($\Sigma 360 \pm 0.06-0.32°$), while the axial positions are occupied by O atoms derived from the dianionic $[RPO_3]^{2-}$ and monoanionic $[RP(OH)O_2]^-$ phosphonate groups [166.72(8)−174.54(8)°] (Figure 3b). The role of the other hydrogenphosphonate moiety (P3) is to provide interchain connectivity via O(P)−H···O hydrogen-bonding interactions involving H9 and O8 atoms and to extend the structure into a 2D motif. The bond parameters involved in these interactions are as follows: O9−H9 = 0.84 Å, H9···O8 = 1.750(2) Å, O9···O8 = 2.574(3) Å; O9−H9···O8 = 167°; symmetry code, $-x$, $-y + 2$, $-z + 1$. The transformation into a 3D structure is effected by participation of the O8 atoms in forming bifurcated hydrogen bonds with the H11 atoms of the hydrogenphosphonate (P4) groups of the adjacent layers [O11−H11 = 0.84 Å, H11···O8 = 1.817(2) Å, O11···O8 = 2.603(3) Å; O11−H11···O8 = 155°; symmetry code, $-x$, $y + {}^1/_2$, $-z + {}^1/_2$] (Figure 3c).

Although the core atom arrangement comprising a $Sn_3P_2O_6$ unit in **4** is similar to that of **3**, the primary structure

Table 7. Selected Bond Lengths (Å) and Bond Angles (deg) for **6**[a]

Sn1−C1	2.093(13)	Sn1−C3	2.121(11)
Sn1−O3^{i}	2.122(8)	Sn1−O1	2.132(8)
Sn1−O8^{i}	2.427(9)	Sn1−O6	2.429(8)
Sn2−C12	2.101(13)	Sn2−C10	2.110(11)
Sn2−O11^{i}	2.121(8)	Sn2−O9	2.130(10)
Sn2−O16^{i}	2.411(9)	Sn2−O14	2.458(9)
O5−C8	1.445(15)	O13−C17	1.468(16)
C1−Sn1−C3	165.3(6)	O3^{i}−Sn1−O8^{i}	86.8(3)
O3^{i}−Sn1−O1	90.9(3)	O8^{i}−Sn1−O6	91.3(3)
O1−Sn1−O6	91.5(3)	C12−Sn2−C10	164.1(5)
O11^{i}−Sn2−O16^{i}	91.6(3)	O16^{i}−Sn2−O14	91.7(4)
O9−Sn2−O14	88.8(3)	O11^{i}−Sn2−O9	88.4(3)

[a] Symmetry transformations used to generate equivalent atoms: i, $x - 1$, y, z.

Table 8. Selected Bond Lengths (Å) and Bond Angles (deg) for **7**[a]

Sn−O1	2.1000(16)	Sn−C1	2.108(3)
Sn−O3^{i}	2.1090(17)	Sn−C5	2.115(3)
Sn−O8^{ii}	2.4641(18)	Sn−O6	2.4822(18)
O5−C12	1.459(5)		
O1−Sn−C1	96.88(9)	C1−Sn−C5	156.99(10)
O1−Sn−O3^{i}	88.54(7)	O1−Sn−O8^{ii}	84.26(7)
O8^{ii}−Sn−O6	101.95(7)	O3^{i}−Sn−O6	85.24(6)

[a] Symmetry transformations used to generate equivalent atoms: i, $-x + {}^1/_2$, $-y + {}^1/_2$, $-z$; ii, $-x + {}^1/_2$, $y + {}^1/_2$, $-z + 1$.

(12) (a) Yasuda, H.; Choi, J.-C.; Lee, S.-C.; Sakakura, T. *J. Organomet. Chem.* **2002**, *659*, 133. (b) Choi, J.-C.; Sakakura, T.; Sako, T. *J. Am. Chem. Soc.* **1999**, *121*, 3793.

(13) Desiraju, G. R.; Steiner, T. *The Weak Hydrogen Bond: In Structural Chemistry and Biology*; Oxford University Press: Oxford, U.K., 1998; p 29.

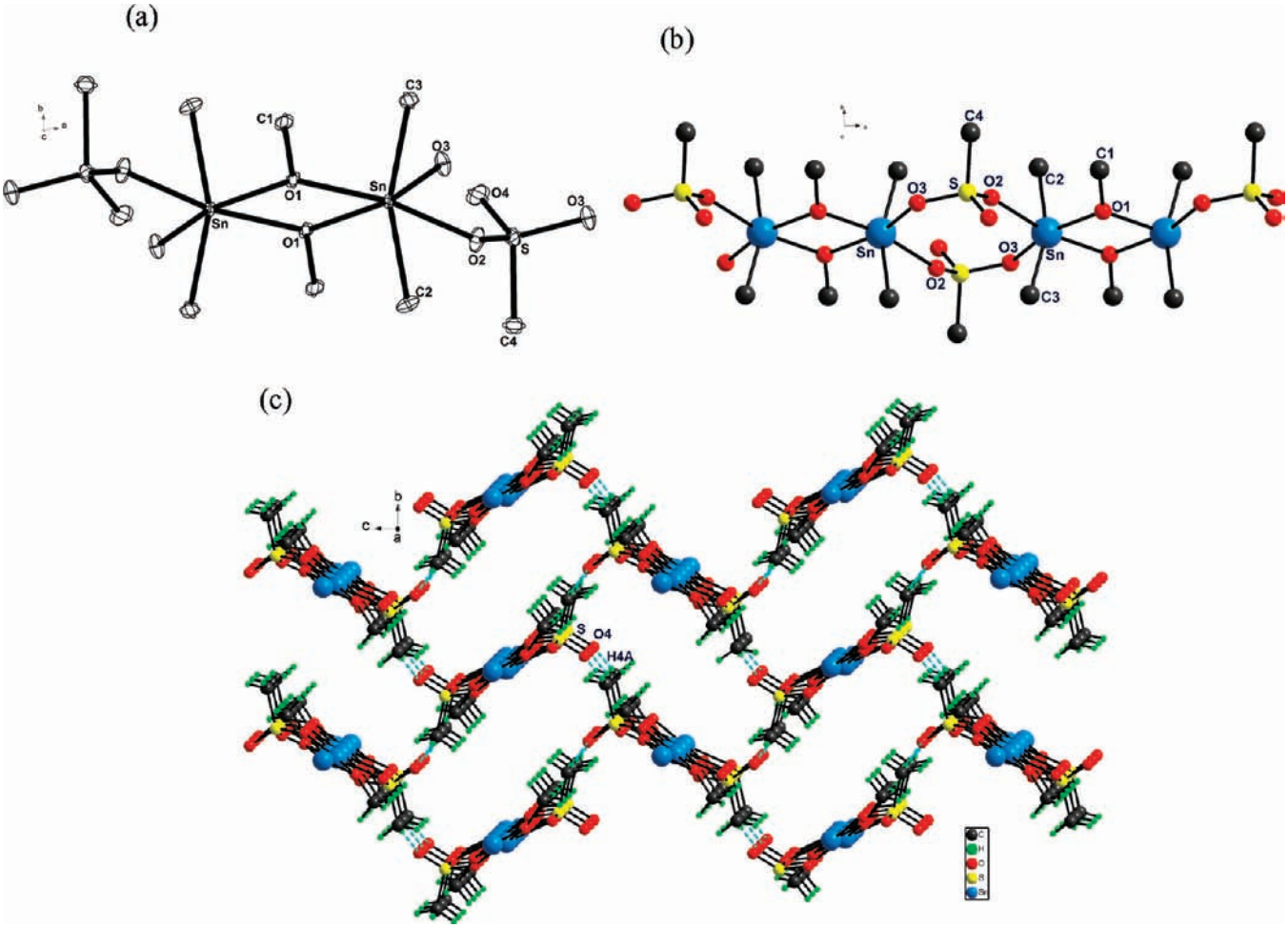

Figure 1. (a) ORTEP view of the asymmetric unit of **1**. The thermal ellipsoids are set at 30% probability, and all of the H atoms are omitted for clarity. (b) 1D structure of **1** along the *a* axis. All of the H atoms are omitted for clarity. (c) 3D structure of **1** viewed along the *a* axis showing intermolecular hydrogen-bonding interactions.

differs with respect to peripheral functionalization of the Sn2 and Sn3 atoms by ethanesulfonate groups (S1 and S2) as well as coordinative association of methanol (O13) to the Sn1 atom (Figure 4a). The presence of appended sulfonate groups and their ability to exhibit variable coordination modes (μ_2 and μ_3) offer knitting tools for the formation of a 3D coordination polymer assembly. The 2D-layered structure comprising large macrocyclic rings (Figure 4b) is effected by μ_2 coordination of O8(S1) and O12(S2) atoms with Sn3 and Sn1 atoms, respectively, of the adjacent units. The sulfonate (S1) groups complete their μ_3 coordination (via O9) and provide connectivity to the layers by association with the (Sn2) atoms, which results in the formation of eight-membered $-[Sn-O-S-O-]_2$ puckered rings (Figure 4c), as were also evident in the structures of **1** and **2**. Each Sn atom in the 3D assembly adopts a distorted octahedral geometry, with the SnO_4 moiety occupying the basal plane [$\Sigma 360 \pm 0.06-0.88°$] and a trans disposition of methyl groups (149.35−156.35°). The Sn−O(P) bond lengths [Sn1−O3 = 2.086(3) Å, Sn1−O5 = 2.075(3) Å, Sn2−O1 = 2.060(2) Å, Sn2−O4 = 2.091(2) Å, Sn3−O2 = 2.081(2) Å, and Sn3−O6 = 2.077(3) Å] lie in the range of Sn−O covalent bonds (2.0−2.1 Å). The Sn−O(S) bond lengths [Sn1−O12^{iii} = 2.578(3) Å, Sn2−O7 = 2.439(3) Å, Sn2−O9^{iv} = 2.777(3) Å, Sn3−O8^{i} = 2.559(3) Å, and Sn3−O10 = 2.542(3) Å] are comparatively large, suggesting appreciable ionic character. The coordinated methanol molecule contributes toward O−H---O-type hydrogen bonding, in which participation of the uncoordinated O11(S2) and methanolic H (H13) atoms is discernible in the structure [O13−H13 = 0.86(3) Å, H13---O11 = 1.83(3) Å, O13···O11 = 2.679(5) Å; O13−H13···O11 = 167(2)°; symmetry code, x, $-y + {}^1/_2$, $z + {}^1/_2$].

X-ray crystal structures of **5**−**7** derived from sulfonate and carboxyphosphonate ligand sets reveal significant variations in their structural characteristics, depending upon the nature of the substituents on tin and/or sulfonate groups. Nevertheless, a common feature in all of these compounds is a facile in situ transformation of the carboxylic functional group to a methyl ester moiety. As a result, the formation of primary structural units is derived from the preferential participation of sulfonate and phosphonate/hydrogenphosphonate ligands, while the ester group remains invariably passive toward coordination.

The asymmetric unit of **5** incorporates the same $Sn_3P_2O_6$ structural framework as those in **3** and **4** but bearing a methanesulfonate group on each of the two Sn1 atoms [Sn1−O7 = 2.362(4) Å]. Its formation from the μ_3-phosphonate [Sn1−O1 = 2.097(3) Å, Sn1−O2^{i} = 2.058(3) Å, and Sn2−O3^{i} = 2.081(3) Å] moiety is similar to that of **4**, while the dangling methylpropionate group on each P atom remains free (Figure 5a). The molecular units are coordinatively

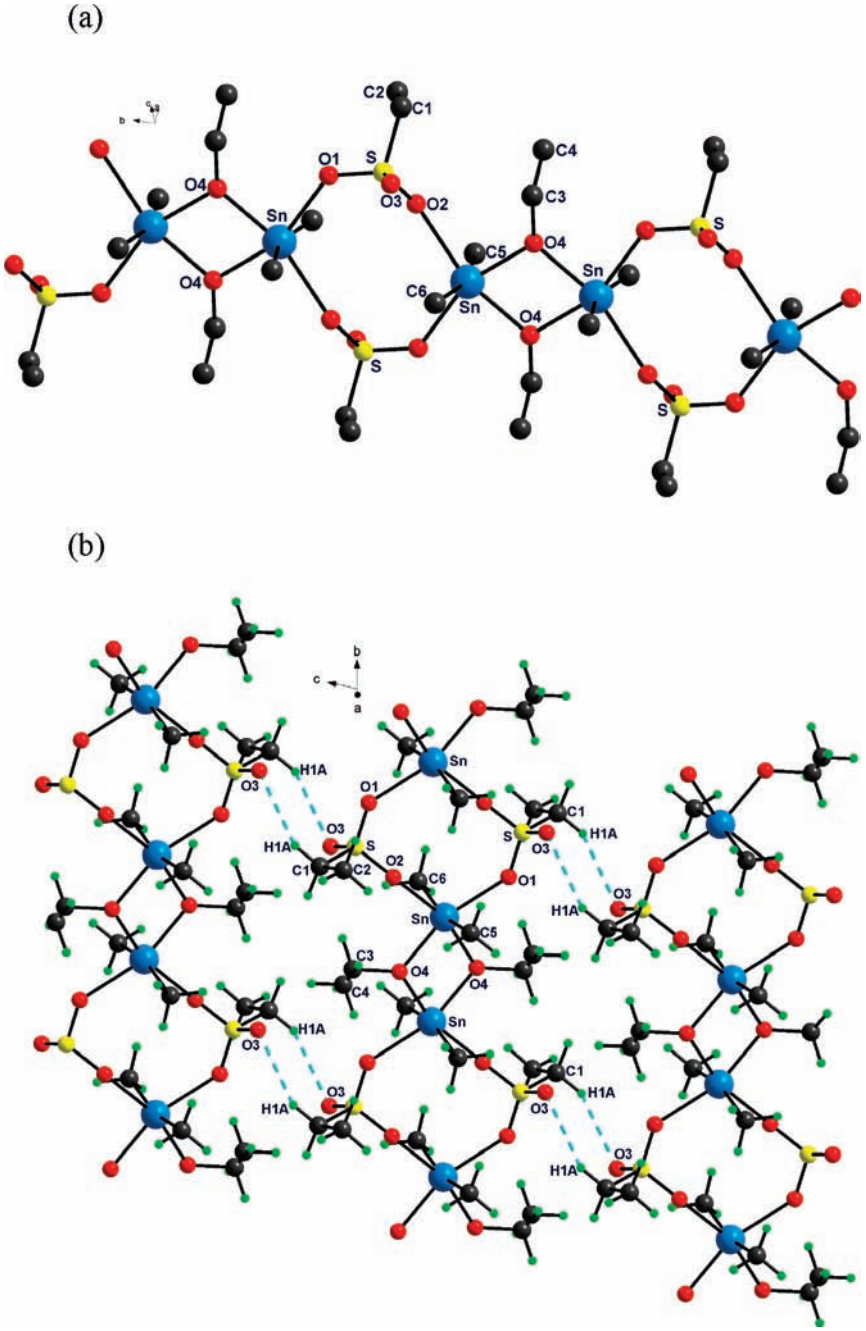

Figure 2. (a) 1D structure of **2** along the *a* axis. All of the H atoms are omitted for clarity. (b) 2D structure of **2** viewed in the *bc* plane showing intermolecular hydrogen-bonding interactions.

associated with one another by involving a O6 atom of each of two symmetry-related sulfonate groups in a μ_2 manner and a Sn2 atom [Sn2−O6 = 2.556(4) Å]. This provides a layered polymer assembly featuring a network of square grids of dimension 10.61 × 10.61 Å in the *ab* plane (Figure 5b). The geometry around each Sn1 atom is five-coordinated, with an SnC_2O core (Σ360 ± 3.05°) forming the equatorial plane and a trans disposition of the O7(S) and O1(P) atoms [∠O1−Sn1−O7 = 168.42(15)°]. The Sn2 atoms possesses a distorted octahedral geometry with a SnO_4 basal plane (Σ360 ± 0.90°) and *trans*-methyl groups [∠C7−Sn1−C7^i = 149.1(3)°]. The S−O bond length associated with an uncoordinated O8(S) atom is shorter (1.45 Å) in comparison to those involved in bonding with the Sn atoms (S−O6 = 1.46; S−O7 = 1.47 Å).

The structure of **6** reveals two independent molecules in the unit cell (designated by Sn1 and Sn2), of which only one is shown in Figure 6a. A unique feature of the structural motif is the involvement of both methanesulfonate and hydrogenphosphonate ligands in bridging bidentate modes to facilitate the formation of 1D polymeric chains, which are composed of repeating eight-membered cyclic rings containing Sn, O, P, and S heteroatoms [Sn−O(P) = 2.121(8)−2.132(8) Å; Sn−O(S) = 2.411(9)−2.458(9) Å]. The composition of the polymer as the one obtained herein is unprecedented because all previously reported examples of similarly related coordination self-assemblies are associated with alternate [−Sn−O−P−O−]$_2$ and −[Sn−O−S−O−]$_2$ rings. Each Sn atom in **6** adopts a distorted octahedral geometry, with an SnO_4

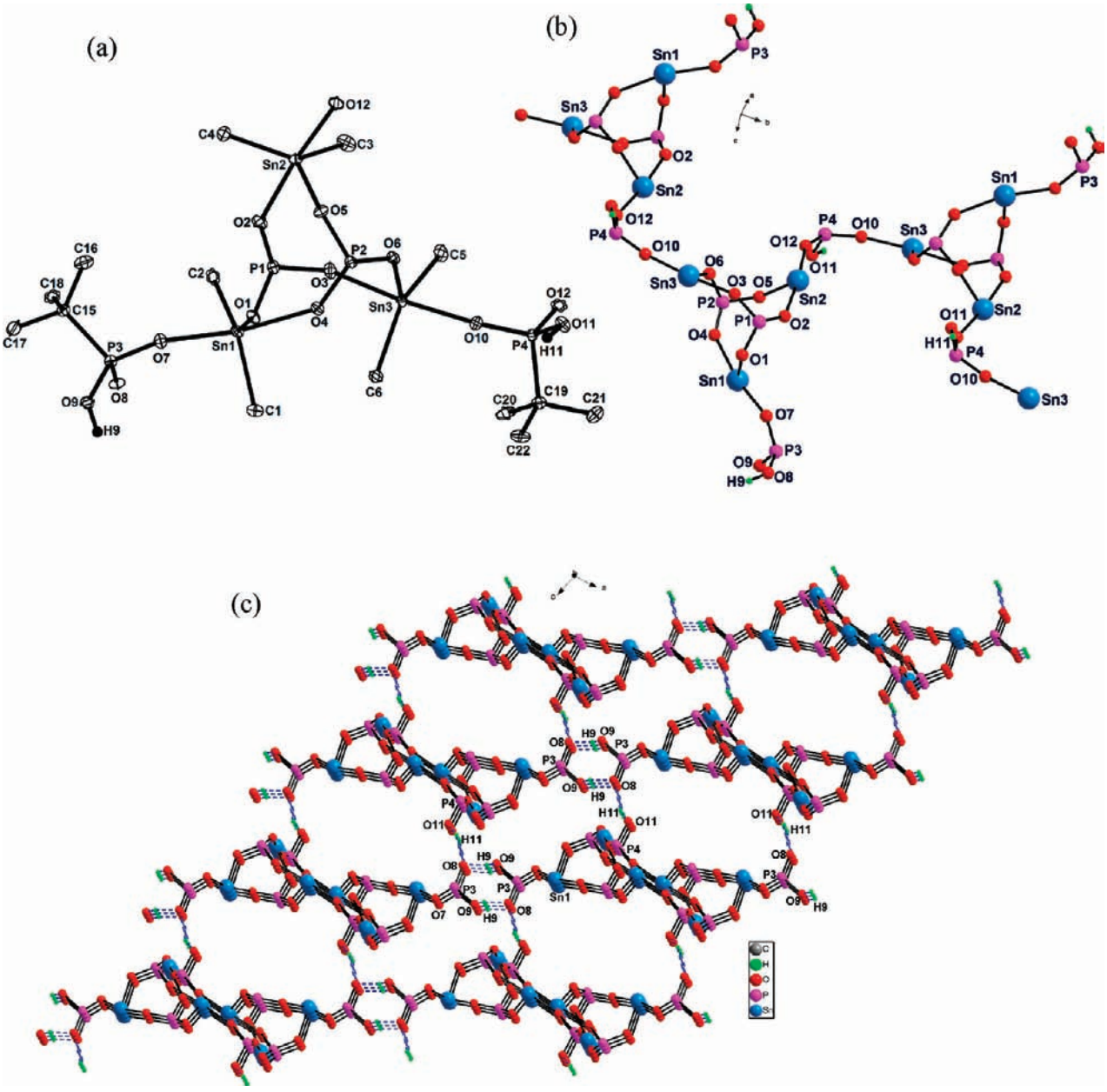

Figure 3. (a) ORTEP view of the asymmetric unit of **3**. The thermal ellipsoids are set at 30% probability. All of the H atoms (except H9 and H11) and *tert*-butyl groups on P1 and P2 atoms are omitted for clarity. (b) 1D structure of **3** along the *b* axis. All of the hydrocarbon groups are omitted for clarity. (c) 3D structure of **3** viewed along the *b* axis. All of the hydrocarbon groups are omitted for clarity. Hydrogen-bonding interactions are shown by dashed lines (blue color).

($\Sigma 360 \pm 0.5°$) core occupying a plane while two ethyl groups are disposed on either side in a trans manner [$\angle$C1−Sn1−C3 = 165.3(6)°; $\angle$C12−Sn2−C10 = 164.1(5)°]. The polymeric chains associated with Sn1 and Sn2 atoms do not exhibit any interactions with each other. However, hydrogen-bonding interactions of the type (P)O−H···O(S) are discernible in crystallographically similar chains, generating parallel, noninteracting sheets incorporating either Sn1 or Sn2. The metrical parameters associated with these bondings are as follows: O2−H2 = 0.84 Å, H2···O7^{i} = 1.747(8) Å, O2···O7^{i} = 2.573(12) Å; O2−H2···O7^{i} = 167.4(7)°; O10−H10 = 0.84 Å, H10···O15^{ii} = 2.290(9) Å, O10···O15^{ii} = 2.584(12) Å; O10−H10···O15^{ii} = 100.9(7)°; symmetry code, i, $x-1, y, z-1$, ii, $x+1, y, z+1$.

The molecular structure of **7** (Figure 7a) corresponds to a centrosymmetric dimer based on an eight-membered ring formed by a bridging bidentate mode of the hydogenphosphonate group. Each Sn atom in the molecule is associated with an appended ethanesulfonate group, which provides a bridging connectivity to the neighboring units and results in the formation of a sheetlike structural motif featuring 24-membered hexatin macrocyclic rings [Sn−O1 = 2.100(16) Å, Sn−O3^{i} = 2.1090(17) Å, Sn−O8^{ii} = 2.4641(18) Å, and Sn−O6 = 2.4822(18) Å] (Figure 7b). Each Sn atom in the extended assembly adopts a distorted octahedral geometry with the basal plane defined by the SnO_4 core ($\Sigma 360 \pm 0.1°$). The *n*-butyl groups adopt a trans disposition with a C−Sn−C angle of 157(1)°. In addition, strong (P)O−H···O (S) hydrogen-bonding interactions between the hydroxyl group and the O atom of adjacent alkanesulfonate groups are evident. Significant metrical parameters associated with these interactions are summarized as follows: [O2−H2 = 0.84 Å, H2···O7 = 1.747(2) Å,

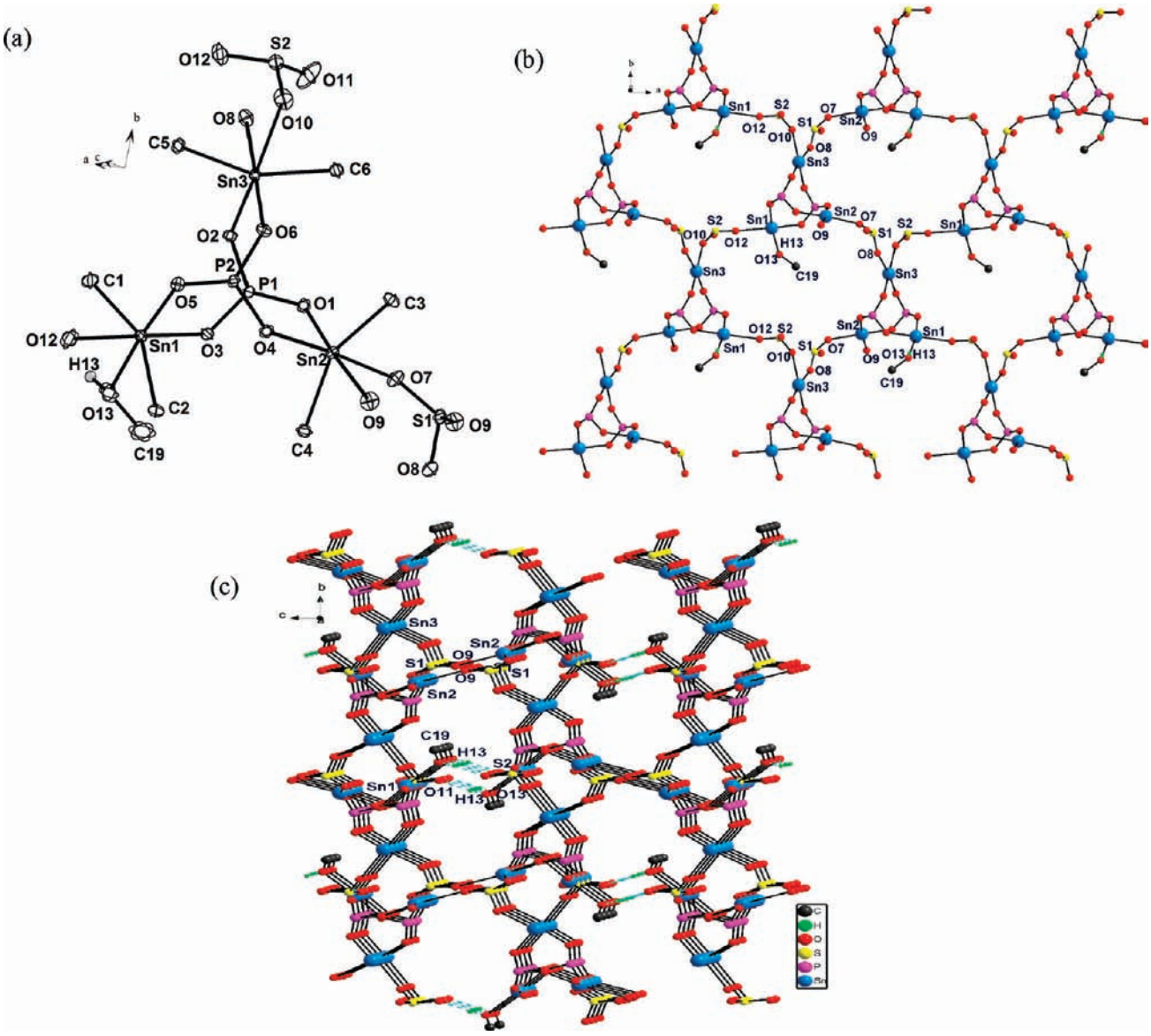

Figure 4. (a) ORTEP view of the asymmetric unit of **4**. The thermal ellipsoids are set at 30% probability. All of the hydrocarbon groups (except Sn−C) are omitted for clarity. (b) 2D structure of **4** in the *ab* plane. All of the hydrocarbon groups are omitted for clarity. (c) 3D structure of **4** viewed along the *a* axis. All of the hydrocarbon groups are omitted for clarity. Hydrogen-bonding interactions are shown by dashed lines (cyan color).

O2···O7 = 2.573(3) Å; O2−H2···O7 = 167.4(1)°; symmetry code, x, $y + 1$, z].

Spectroscopic Studies. The compounds **3**−**7** are only soluble in coordinating solvents such as CH_3OH and dimethyl sulfoxide (DMSO). As a result, NMR spectra have been studied in DMSO-d_6, and the relevant data are summarized in the Experimental Section. It is imperative to mention that the presence of weakly coordinating sulfonate groups and noncovalent hydrogen-bonding interactions associated with the self-assemblies and their likely dissociation in donor solvents[14] allow only a qualitative interpretation regarding the true nature of the organotin species present in solution.

The ^1H and $^{13}C\{^1H\}$ NMR spectra are well-resolved and provide a good estimate of the composition of each compound. For **5**−**7**, the spectral studies also validate the formation of a methyl ester functionality on the P atom [^1H: δ 3.58−3.61 (OCH_3); $^{13}C\{^1H\}$: δ 51.70−51.72 (OCH_3), 172.63−172.83 (CO_2)]. The retention of a trinuclear tin phosphonate structure in **3**−**5** is confirmed by the observed heteronuclear $^2J_{Sn-O-P}$ = 240−251 Hz coupling in both ^{31}P and ^{119}Sn NMR spectra and the triplet nature of the tin spectrum. For **3**, the appearance of two ^{31}P signals at δ 30.54 (br) and 25.73 (s, $^2J_{Sn-O-P}$ = 248 Hz) is in accordance with the presence of monoanionic hydrogenphosphonate and dianionic phosphonate groups in the framework, consistent with the X-ray crystal structure. On the other hand, the spectral features of **6** and **7** are broad and devoid of heteronuclear $^2J_{Sn-O-P}$ coupling information. These results find analogy with our previous studies on related diorganotin derivatives, which are composed of [−Sn−O−P−O−]$_2$ and [−Sn−O−S−O−]$_2$

(14) (a) Holeček, J.; Nadvorník, M.; Handlír, K.; Lyčka, A. *J. Organomet. Chem.* **1986**, *315*, 299. (b) Gross, D. C. *Inorg. Chem.* **1989**, *28*, 2355. (c) Dakternieks, D.; Jurkschat, K.; Dreumel, S. V. *Inorg. Chem.* **1997**, *36*, 2023. (d) Narula, S. P.; Kaur, S.; Shankar, R.; Verma, S.; Venugopalan, P.; Sharma, S. K. *Inorg. Chem.* **1999**, *38*, 4777.

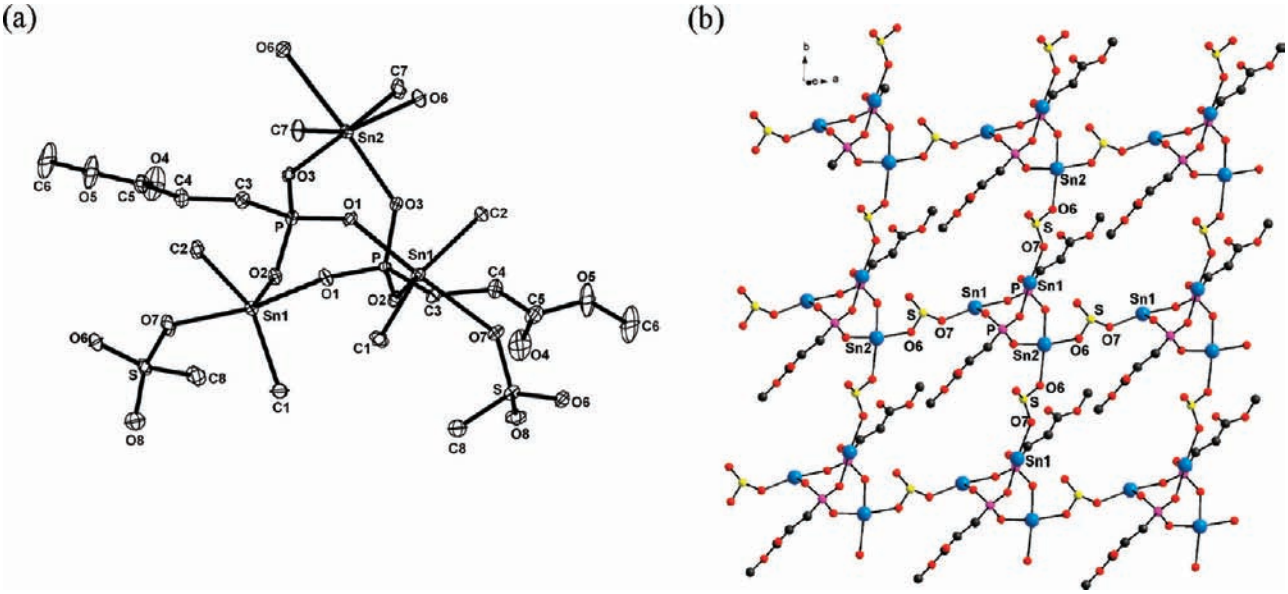

Figure 5. (a) ORTEP view of **5**. The thermal ellipsoids are set at 30% probability. All of the H atoms are omitted for clarity. (b) 2D structure of **5**. All of the H atoms and methyl groups attached to Sn and S atoms are omitted for clarity.

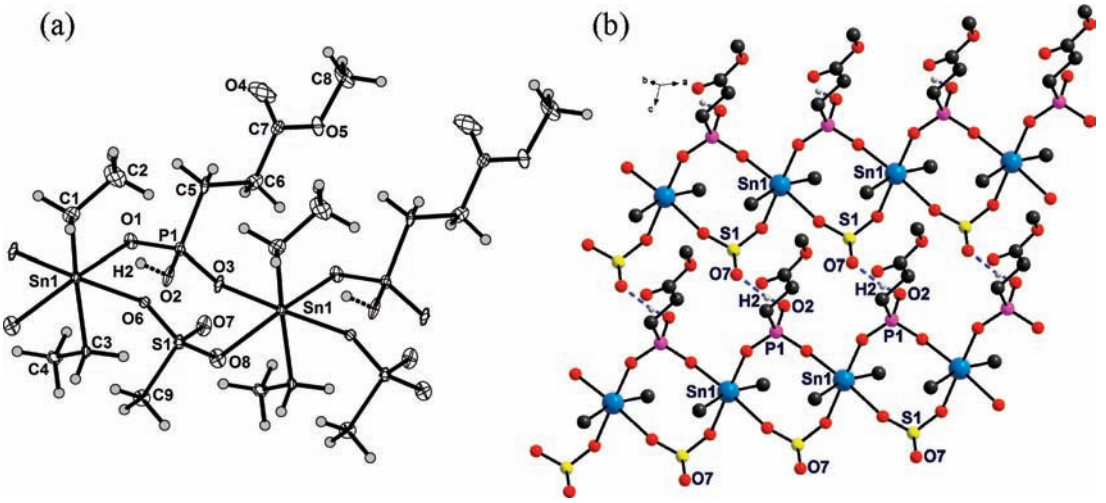

Figure 6. (a) ORTEP view of **6**. The thermal ellipsoids are set at 30% probability. (b) 2D structure of **6** showing intermolecular hydrogen-bonding interactions. All of the H (except H2) and C atoms attached to Sn [except Sn−C(α)] and S atoms are omitted for clarity.

ring systems[10a,b] and suggest dissociation of the network structures of the coordination polymers to yield an equilibrium mixture of different organotin species. The ^{119}Sn chemical shifts (δ −293 to −393) as well as $^{1}J_{Sn-C}$ coupling values (965−1036 Hz) of all of the compounds fall in the range of six-coordinated Sn atoms, as is expected in DMSO-d_6, which provides coordinative saturation to the tin centers even where lattice dissociation has occurred. The IR spectral region of 940−1200 cm^{-1} is associated with overlapped stretching vibrations of the PO_3 and SO_3 groups and is thus not informative in evaluating the coordination modes of these ligands. For **5**−**7**, the presence of a methyl ester moiety is evident from the characteristic IR absorption at 1730−1745 cm^{-1}.

In conclusion, the results described herein demonstrate the versatility of diorganotin(alkoxy)alkanesulfonates as precursors for the synthesis of novel coordination polymers **3**−**7** incorporating alkanesulfonate/phosphonate/carboxyphosphonate ligands in the structural frameworks. The formation of **3** and **4** results from SBUs that are comprised of trinuclear tin phosphonate entities, $[(R_2Sn)_3(O_3PBu^t)_2L_2]$ [L = $O_2P(OH)Bu^t$, OSO_2Et]. These results implicate the role of solvent in executing the transformation of a functional group (L) in these SBUs. For **5**−**7**, in situ formation of the ester moieties seems to be significant in protecting the otherwise potential donor sites of the carboxylate groups and allows the construction of 2D assemblies with the aid of phosphonate and sulfonate moieties. Further studies are in progress to harness the coordination properties of bifunctional phosphonocarboxylic acids in organotin chemistry.

Experimental Section

All operations were carried out using standard Schlenk-line techniques under a dry nitrogen atmosphere. Solvents were freshly distilled over phosphorus pentoxide (dichloromethane, chloroform, acetonitrile, and hexane), sodium wire (diethyl ether), and magnesium cake (methanol). Glassware

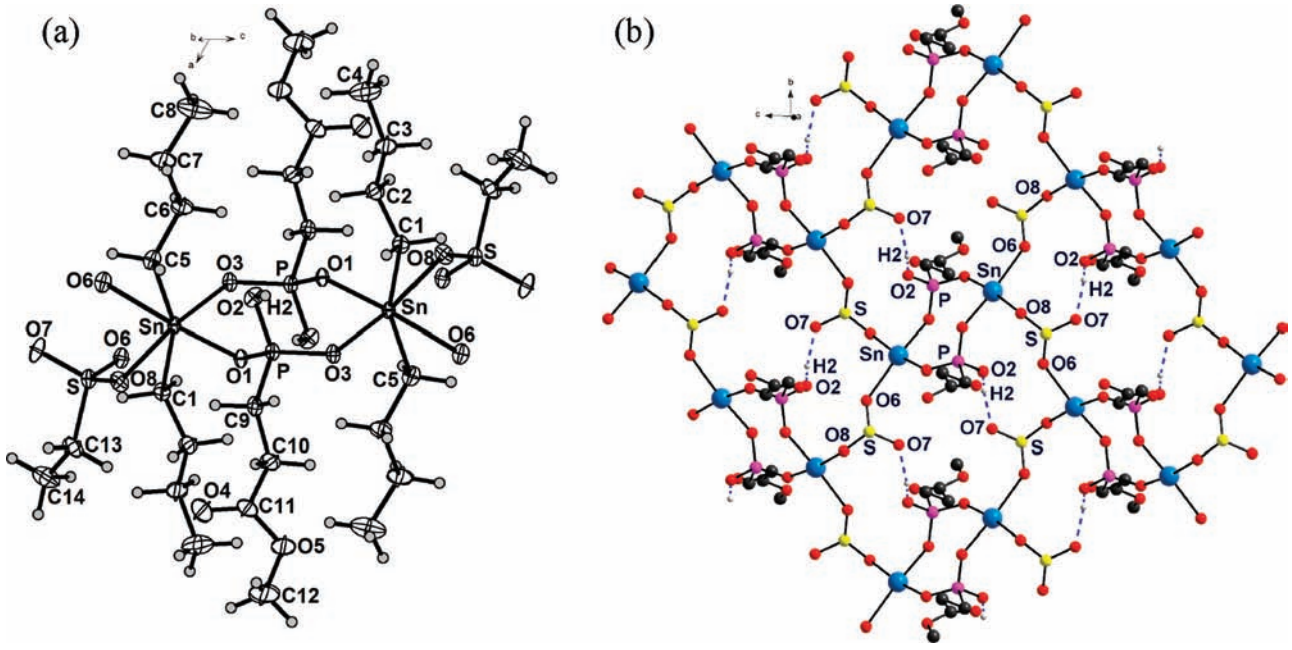

Figure 7. (a) ORTEP view of **7**. The thermal ellipsoids are set at 30% probability. (b) 2D structure of **7** showing intermolecular hydrogen-bonding interactions. All of the H (except H2) and C atoms attached to Sn and S atoms are omitted for clarity.

was dried in an oven at 110−120 °C and further flame-dried under vacuum prior to use. ^{1}H, ^{13}C{^{1}H}, ^{31}P, and ^{119}Sn NMR spectra were recorded on a Bruker DPX-300 spectrometer at 300, 75.47, 121.50, and 111.88 MHz, respectively. ^{1}H and ^{13}C chemical shifts are quoted with respect to the residual protons of the solvent, while ^{119}Sn and ^{31}P NMR data are given using tetramethyltin and 85% H_3PO_4 as external standards, respectively. IR spectra were recorded on a Nicolet protege 460 ESP spectrophotometer using KBr optics. Elemental analysis (C and H) was performed on a Perkin-Elmer model 2400 CHN elemental analyzer. The tin precursors, dialkyltin(alkoxy)-alkanesulfonates, were prepared by literature procedures.[10]

Synthetic Methods. Synthesis of $[(Me_2Sn)_3(O_3PBu^t)_2(O_2P(OH)Bu^t)_2]_n$ (3). To a solution of the tin precursor, either $[Me_2Sn(OMe)(OSO_2Me)]_n$ (**1**; 0.45 g, 1.64 mmol) or $[Me_2Sn(OEt)(OSO_2Et)]_n$ (**2**; 0.50 g, 1.64 mmol) in methanol (40 mL), which was kept under an inert atmosphere, was added an equimolar quantity of *tert*-butylphosphonic acid (0.26 g, 1.64 mmol) at room temperature with constant stirring. A clear solution was obtained and was stirred for 8−10 h. Thereafter, the solution was concentrated and left open to the air for crystallization. A crop of colorless crystals was obtained and identified as **3**. Yield: 0.38 g, 69%. ^{1}H NMR (DMSO-d_6): δ 0.82 (s, $^{2}J_{Sn-H}$ = 108.6 Hz, 18H, SnCH_3), 1.09 (d, $^{2}J_{P-H}$ = 16.50 Hz, 18H, $O_3PC(CH_3)_3$), 1.01 (d, $^{2}J_{P-H}$ = 15.90 Hz, 18H, $O_2P(OH)C(CH_3)_3$). ^{13}C{^{1}H} NMR (DMSO-d_6): δ 30.82 (d, $^{1}J_{P-C}$ = 150 Hz, $O_3PC(CH_3)_3$), 30.42 (d, $^{2}J_{P-C}$ = 145 Hz, $O_2P(OH)C(CH_3)_3$), 24.98 (PC(CH_3)$_3$), 13.64 (SnCH_3). ^{119}Sn NMR (DMSO-d_6): δ −317.48 (t, $^{2}J_{Sn-O-P}$ = 251 Hz). ^{31}P NMR (DMSO-d_6): δ 30.54 (br, $O_2P(OH)Bu^t$), 25.73 (s, $^{2}J_{Sn-O-P}$ = 248 Hz). IR (KBr, cm^{-1}): 1102, 936 [$\nu(PO_3)$], 2368 [ν(PO−H], hydrogen-bonded). Anal. Calcd for $C_{22}H_{56}O_{12}P_4Sn_3$: C, 26.62; H, 5.69. Found: C, 26.60; H, 5.70.

Synthesis of $[(Me_2Sn)_3(O_3PBu^t)_2(OSO_2Et)_2\cdot MeOH]_n$ (4). To a solution of dimethyltin(ethoxy)ethanesulfonate (**2**; 0.50 g, 1.65 mmol) in dry dichloromethane (30 mL) was added *tert*-butylphosphonic acid (0.23 g, 1.65 mmol), and the contents were stirred for 8 h at room temperature. A white solid thus obtained was filtered, washed with hexane, and dried under vacuum. Recrystallization of the solid by the slow diffusion of diethyl ether into a $CHCl_3/CH_3OH$ solvent mixture afforded **4** in analytically pure form. Yield: 0.37 g, 68%. ^{1}H NMR (DMSO-d_6): δ 3.24 (d, 3H, CH_3OH), 2.45 (q, $^{3}J_{H-H}$ = 7.5 Hz, 4H, SCH_2CH$_3$), 1.20 (d, $^{2}J_{P-H}$ = 16.20 Hz, 18H, PC(CH_3)$_3$), 1.13 (t, $^{3}J_{H-H}$ = 7.5 Hz, 6H, SCH$_2$CH_3), 0.92 (s, $^{2}J_{Sn-H}$ = 108 Hz, 18H, SnCH_3). ^{13}C{^{1}H} NMR (DMSO-d_6): δ 54.96 (CH_3OH), 45.27 (SCH_2CH$_3$), 30.84 (d, $^{1}J_{P-C}$ = 150 Hz, PC(CH$_3$)$_3$), 25.12 (PC(CH_3)$_3$), 13.53 ($^{1}J_{Sn-C}$ = 998 Hz, SnCH_3), 9.90 (SCH$_2$CH_3). ^{119}Sn NMR (DMSO-d_6): δ −293.07 (t, $^{2}J_{Sn-O-P}$ = 242 Hz). ^{31}P NMR (DMSO-d_6): δ 26.22 (s, $^{2}J_{Sn-O-P}$ = 240 Hz). IR (KBr, cm^{-1}): 1260, 1201, 1091, 1014 [$\nu(SO_3) + \nu(PO_3)$], 2363 [ν(PO−H], hydrogen-bonded), 3404 [ν(CH$_3$OH)]. Anal. Calcd for $C_{19}H_{50}O_{13}P_2S_2Sn_3$: C, 23.56; H, 5.20. Found: C, 23.54; H, 5.16.

Synthesis of 5−7. To a suspension of the tin precursor, either $[Me_2Sn(OMe)(OSO_2Me)]_n$ (**1**; 0.65 g, 2.36 mmol), $[Et_2Sn(OMe)(OSO_2Me)]_n$ (0.72 g, 2.36 mmol), or $[^nBu_2Sn(OEt)(OSO_2Et)]_n$ (0.91 g, 2.36 mmol) in methanol (40 mL) was added 3-phosphonopropranoic acid (0.36 g, 2.36 mmol) at room temperature with constant stirring. After 8−10 h, the clear solution was concentrated under vacuum and *n*-hexane was added to precipitate a white solid in each case. The solid thus obtained was filtered, dried under vacuum, and recrystallized from an acetonitrile−methanol mixture to yield **5**−**7**, respectively.

$[(Me_2Sn)_3(O_3PCH_2CH_2COOMe)_2(OSO_2Me)_2]_n$ (5). Yield: 0.61 g, 80%. ^{1}H NMR (DMSO-d_6): δ 3.61 (s, 6H, OCH$_3$), 2.47 (t, $^{3}J_{H-H}$ = 8.2 Hz, 4H, PCH$_2$CH_2), 2.31 (s, 6H, SCH$_3$), 1.84−1.79 (m, 4H, PCH_2CH$_2$), 0.83 (s, 18H, (CH_3)$_2$Sn). ^{13}C-{^{1}H} NMR (DMSO-d_6): δ 172.83, 172.55 (CO_2), 51.70 (OCH$_3$), 39.50 (SCH$_3$, merged in a DMSO peak), 28.13 (PCH$_2$CH_2), 24.02 (d, $^{2}J_{P-C}$ = 152 Hz, PCH$_2$CH$_2$), 14.12 ($^{1}J_{Sn-C}$ = 965 Hz (CH_3)$_2$Sn). ^{119}Sn NMR (DMSO-d_6): δ −326.86 (t, $^{2}J_{Sn-O-P}$ = 246 Hz). ^{31}P NMR (DMSO-d_6): δ 18.36 (s, $^{2}J_{Sn-O-P}$ = 242 Hz). IR (KBr, cm^{-1}): 1201, 1097, 1048, 1010 [$\nu(SO_3) + \nu(PO_3)$], 1738 [$\nu(CO_2)$]. Anal. Calcd for $C_{16}H_{32}O_{16}P_2S_2Sn_3$: C, 19.96; H, 3.35. Found: C, 19.95; H, 3.33.

$[Et_2Sn(O_2P(OH)CH_2CH_2COOMe)(OSO_2Me)]_n$, 6. Yield: 0.96 g, 92%. ^{1}H NMR (DMSO-d_6): δ 3.60 (s, 6H, OCH_3), 2.48 (t, $^{3}J_{H-H}$ = 8.2 Hz, 4H, PCH$_2$CH_2), 2.41 (s, 6H, SCH_3), 1.89−1.79 (m, 4H, PCH_2CH$_2$), 1.43 (q, $^{3}J_{H-H}$ = 7.5 Hz, 8H, CH$_3$CH_2Sn), 1.24 (t, 12H, $^{3}J_{H-H}$ = 6.6 Hz, CH_3CH$_2$Sn). ^{13}C-{^{1}H} NMR (DMSO-d_6): δ 172.89, 172.63 (CO_2), 51.70 (OCH$_3$),

39.50 (SCH_3, merged in a DMSO peak), 27.94 (PCH_2CH_2), 23.45 (d, $^2J_{P-C} = 146$ Hz, PCH_2CH_2), 26.36 ($^1J_{Sn-C} = 1036$ Hz, CH_3CH_2Sn), 10.03 ($^2J_{Sn-C} = 53$ Hz, CH_3CH_2Sn). ^{119}Sn NMR (DMSO-d_6): δ −394.94. ^{31}P NMR (DMSO-d_6): δ 18.98 (br). IR (KBr, cm^{-1}): 1200, 1122, 1050 [$\nu(SO_3) + \nu(PO_3)$], 1738 [$\nu(CO_2)$]. Anal. Calcd for $C_9H_{21}O_8PSSn$: C, 24.62; H, 4.82. Found: C, 24.60; H, 4.83.

[^{n}Bu$_2$Sn(O$_2$P(OH)CH$_2$CH$_2$COOMe)(OSO$_2$Et)]$_n$ (7). Yield: 1.12 g, 93%. ^{1}H NMR (DMSO-d_6): δ 3.58 (6H, OCH_3), 2.54−2.43 (m, 8H, $PCH_2CH_2 + SCH_2$), 1.88−1.76 (m, $^3J_{H-H}$ = 8.4 Hz, 4H, PCH_2CH_2), 1.58 (br, 8H, $SnCH_2$), 1.40 (br, 8H, $SnCH_2CH_2$), 1.26 (sext, $^3J_{H-H}$ = 7.2 Hz, 8H, $CH_2(CH_2)_2Sn$), 1.07 (t, $^3J_{H-H}$ = 7.2 Hz, 6H, CH_3CH_2S), 0.88 (t, $^3J_{H-H}$ = 7.2 Hz, 12H, $CH_3(CH_2)_3Sn$). ^{13}C{^{1}H} NMR (DMSO-d_6): δ 172.85, 172.58 (CO_2), 51.72 (OCH_3), 45.34 (SCH_2), 33.08 ($SnCH_2$), 27.92 (PCH_2CH_2), 27.14 ($SnCH_2CH_2$), 25.97 ($Sn(CH_2)_2CH_2$), 23.48 (d, $^2J_{P-C}$ = 146 Hz, PCH_2CH_2), 13.65 ($Sn(CH_2)_3CH_3$), 9.76 (CH_3CH_2S). ^{119}Sn NMR (DMSO-d_6): δ −332.40 (br). ^{31}P NMR (DMSO-d_6): δ 18.10 (br). IR (KBr, cm^{-1}): 1250, 1186, 1062 [$\nu(SO_3) + \nu(PO_3)$], 1744 [$\nu(CO_2)$]. Anal. Calcd for $C_{14}H_{31}O_8PSSn$: C, 33.03; H, 6.14. Found: C, 33.02; H, 6.12.

(15) *HKL DENZO and SCALEPACK*, version l.96: Otwinowski, Z; Minor, W. Macromolecular Crystallography. *Processing of X-ray Diffraction Data Collected in Oscillation Mode; Methods in Enzymology*; Carter, C. W., Jr., Sweet, R. M., Eds.; Acedemic Press: San Diego, CA, 1997; Vol. *276*, Part A, p 307.

(16) Altomare, A.; Burla, M. C.; Carnalli, M.; Cascarano, G.; Giacovazzo, C.; Guagliardi, A.; Moliterni, A. G. G.; Polidori, G.; Spagan, R. *J. Appl. Crystallogr*. **1999**, *32*, 115.

(17) Sheldrick, G. *SHELXL-97, Program for Crystal Structure Refinement*; Institüt für Anorganische Chemie der Unversität Göttingen: Göttingen, Germany, 1997.

X-ray Crystallographic Data. The intensity data for **1**−**7** were collected on a Nonius Kappa CCD diffractometer equipped with a molybdenum-sealed tube and a highly oriented graphite monochromator at 150(2) K by ω, ϕ, and 2θ rotation at 10 s frame^{-1}. Cell parameters, data reduction, and absorption corrections were performed with Nonius software (*DENZO* and *SCALEPACK*).[15] The structures were solved by direct methods using *SIR-97*[16] and refined by a full-matrix least-squares method on F^2 using *SHELXL-97*.[17] All calculations and graphics were performed using *WinGx*.[18] Partial atoms were refined isotropically. All of the non-H atoms were refined anisotropically. H atoms were placed in geometrically calculated positions by using a riding model, except the methanolic hydrogen (H13) in **4**, which was located and refined.

Acknowledgment. This research was supported by grants from CSIR and DST (India). We thank UGC for providing a Senior Research Fellowship to A.J.

Supporting Information Available: Crystallographic data in CIF format. This material is available free of charge via the Internet at http://pubs.acs.org. Crystallographic data for **1** (CCDC 791365), **2** (CCDC 791366), **3** (CCDC 791367), **4** (CCDC 791368), **5** (CCDC 791369), **6** (CCDC 791370), and **7** (CCDC 791371) have been deposited with the Cambridge Crystallographic Data Centre. Copies of this information may be obtained from the Director, CCDC, 12 Union Road, Cambridge CB21EZ, U.K. (fax +44-1233-336033; e-mail deposit@ccdc.cam.ac.uk, or web site www.ccdc.cam.ac.uk).

(18) Farrugia, L. J. *J. Appl. Crystallogr*. **1999**, *32*, 837.